A Double Projection Method for Incompressible Viscoelastic Flow

Sorin M. Mitran & Lingxing Yao

Applied Mathematics Program

Department of Mathematics

University of North Carolina

Chapel Hill 27599-3250

November 1, 2007

Abstract

Incompressible viscoelastic fluids cannot sustain longitudinal wave modes. The incompressibility condition imparts an overall elliptic constraint on the system of partial differential equations describing the flow. To avoid the computational expense of simultaneously solving for fluid velocities and stresses, splitting procedures are widely used in numerical simulations. A common approach is to enforce the elliptic constraint at the end of a computational time step through a projection method. The polymeric stress equation is typically advanced in

time before the constraint is applied. The numerical discretization of the polymeric stress equation can introduce spurious longitudinal modes. The longitudinal modes appear as a spurious excitation of the velocity field when used in the momentum update. To eliminate the spurious modes a double projection method is introduced in the context of a splitting procedure for the Oldroyd-B model. The hyperbolic subsystem capturing shear wave propagation and convective effects is first advanced in time using a wave propagation algorithm, thus obtaining interim velocity and stress values. The stress field is decomposed into divergence-free and force-carrying parts. The deformation field producing the forces is computed. A first projection step is applied to the deformation field to render it divergence-free. The velocity and stress fields are subsequently corrected to remove spurious longitudinal modes. A Helmholtz decomposition is applied to the velocity field and a second projection step is applied to enforce the incompressibility constraint. Though presented for Oldroyd-B fluids, the procedure is general in nature and the correction of interim values of viscoelastic stress can be incorporated in other algorithms used for simulation of incompressible viscoelastic fluids with differential constitutive laws. Example computations are presented for a cavity flow. The spurious forces observed in the interim step of the splitting procedure are shown.

Keywords Viscoelastic flow; Spurious computational modes; Projection method

1 Introduction

We present a description of possible numerical artefacts in the numerical computation of incompressible viscoelastic fluids described by differential constitutive laws, and introduce a procedure to eliminate spurious effects. The system of partial differential equations (PDEs) describing such flows is subject to an elliptic constraint due to the incompressibility condition. The incompressibility condition implies a divergence-free velocity field. The situation is reminiscent of the case of incompressible Newtonian flow and the projection method of Chorin [3] and Temam [17] is commonly applied, e.g. [18]. However, the situation for viscoelastic fluids is different from that for Newtonian fluids. In a Newtonian fluid the incompressibility constraint prohibits propagating pressure waves. The pressure appears as a scalar Lagrangian multiplier for the equations, and the incompressibility constraint can be enforced by solving a single scalar equation. In a viscoelastic fluid the longitudinal modes involve both the pressure and the additional viscoelastic stress. It would be fortuitous for the correction of a stress field to enforce incompressibility to be accomplished by a single scalar function. Indeed, we show below that this is not the case and a vector correction is needed.

The paper is organized as follows. The equations describing the Oldroyd-B physical model are presented in Section 2. We also briefly recall the equations pertaining to Newtonian fluids and Hookean solids. The equations are presented in both a global, fixed Eulerian frame of reference suitable for

numerical modeling and also in a Lagrangian frame of reference with coordinates following the material's deformation as initially suggested by Hencky [6]. The link between the two formulations is provided by the Oldroyd theorem [13] and is useful in understanding the physical constraints that must be satisfied by the evolution in time of the viscoelastic fluid. In Section 3 a numerical method is introduced for the Oldroyd-B system. In common with a number of approaches (e.g. [7],[18], p. 156 of [15]) a splitting procedure is used to avoid the computational expense of simultaneously solving for the pressure, velocity and stress field. The hyperbolic subsystem formed from the momentum equations with no pressure term and the viscoelastic stress transport equation is advanced in time using the wave propagation algorithm of LeVeque [8]. We show that the provisional stress field obtained at this stage contains spurious longitudinal modes which act as a nonphysical force on the system. Furthermore we show that the standard projection approach of correcting the velocity field does not eliminate the spurious forces. In Sect. 4 the Double Projection Method (DPM) is presented. A decomposition of the stress tensor is introduced and the deformation field producing the stress is computed. The deformation field is projected onto a divergence-free subspace. This allows a correction of the interim velocity and stress fields that eliminates any spurious longitudinal wavemodes. A second projection follows the original Chorin [3] procedure and enforces the divergence-free condition on the velocity. We present sample computations for cavity flows in Sect. 5 and compare DPM predictions with those from the standard projection

approach. In particular, numerical experiments show that the double projection procedure stabilizes computations at high Weissenberg numbers for which the standard projection method fails. We close with remarks on the general validity of the procedure for other classes of viscoelastic liquids.

2 Physical model

The modeling of general viscoelastic flows is qualitatively different from the limiting cases of Newtonian fluids and Hookean solids in that the stress-strain relationship is not necessarily instantaneous in time. In general, an integral relation links the time history of the viscoelastic deformation to the stress in the material. A common model exhibiting this dependence is the linear Lodge [9] model,

$$\tau_{xy}(y,t) = \int_{-\infty}^{t} G(t-t') \frac{\partial v_x}{\partial y}(y,t') dt', \tag{1}$$

expressed here in a simple one-dimensional setting with $v_x(y,t)$ a velocity component of the fluid and $\tau_{xy}(y,t)$ the shear stress. Note that for $G(t-t') = \mu\ \delta(t-t')$ one obtains the Newtonian fluid model

$$\tau_{xy}(y,t) = \mu \frac{\partial v_x}{\partial y}(y,t)\ . \tag{2}$$

In this simple case the stress can be deduced from the velocity field at a single time. A key observation is that for general Green's functions $G(t)$ the

time history of the flow would appear. The time history dependence can be modeled either through integro-differential or differential equations.

2.1 Lagrangian and Eulerian descriptions

Rheology seeks to study the behavior of specific viscoelastic flow models [11]. It is typically much easier to derive viscoelastic models that capture some desired real material behavior in a Lagrangian system of coordinates that moves and deforms with the material. This approach was proposed by Hencky [6] and used with great efficacy by Oldroyd [13] and Lodge [10]. Oldroyd set out the general principle that in the coordinate system $(\vec{\xi}, t)$ moving and deforming with the material a constitutive law describing the material can be written as an invariant set of integro-differential equations that link the stress tensor $\boldsymbol{\pi}(\vec{\xi}, t)$, the metric tensor of the co-moving coordinate system $\boldsymbol{\gamma}(\vec{\xi}, t)$, the temperature $T(\vec{\xi}, t)$ and a number of material constants $\kappa(\vec{\xi})$ that depend only on spatial position. Lagrangian time derivatives of these quantities in the co-moving coordinate system are allowed since they do not introduce any spatial dependence. Coordinate derivatives $\partial/\partial\xi^i$ in general cannot appear in the constitutive laws since their presence would introduce a spatial dependence and the stresses should depend on deformation but not on position. Invariant combinations of spatial derivatives are allowed.

Oldroyd proceeds to obtain the transformation of tensor quantities $\boldsymbol{\beta}$ expressed in the co-moving, co-deforming Lagrangian reference frame $(\vec{\xi}, t)$

to a tensor $\boldsymbol{b}$ in the fixed Eulerian frame $(\vec{x}, t)$

$$\beta^{j_1 \ldots j_q}_{i_1 \ldots i_p}(\vec{\xi}, t) = \left| \frac{\partial \vec{x}}{\partial \vec{\xi}} \right|^W \frac{\partial x^{l_1}}{\partial \xi^{i_1}} \ldots \frac{\partial x^{l_p}}{\partial \xi^{i_p}} \ \frac{\partial \xi^{j_1}}{\partial x^{m_1}} \ldots \frac{\partial \xi^{j_q}}{\partial x^{m_q}} b^{m_1 \ldots m_q}_{l_1 \ldots l_p}(\vec{x}, t), \tag{3}$$

where W, the exponent of the inverse Jacobian determinant $J = \left| \partial \vec{x} / \partial \vec{\xi} \right|$, is the weight of the tensor $\boldsymbol{\beta}$. In this and the following we use the repeated index summation convention. Tensor components in the Lagrangian frame are expressed with reference to directions induced by the metric $\boldsymbol{\gamma}$. When transforming a Lagrangian time derivative from the moving frame variations induced by changes in the basis vectors must be taken into account. This is captured by the following principle set out by Oldroyd: wherever a Lagrangian time derivative of a tensor $\boldsymbol{\beta}$ $(\vec{\xi}, t)$ appears in the moving frame, it is replaced in the fixed Eulerian frame by the following derivative of the transformed tensor from (3)

$$\frac{\delta b^{k_1 \ldots k_r}_{i_1 \ldots i_p}}{\delta t} = \frac{\partial b^{k_1 \ldots k_r}_{i_1 \ldots i_p}}{\partial t} + v^m \frac{\partial b^{k_1 \ldots k_r}_{i_1 \ldots i_p}}{\partial x^m} + W \frac{\partial v^m}{\partial x^m} b^{k_1 \ldots k_r}_{i_1 \ldots i_p} \tag{4}$$

$$+ \frac{\partial v^m}{\partial x^{i_1}} b^{k_1 \ldots k_r}_{m \ldots i_p} + \ldots + \frac{\partial v^m}{\partial x^{i_p}} b^{k_1 \ldots k_r}_{i_1 \ldots m} \tag{5}$$

$$- \frac{\partial v^{k_1}}{\partial x^m} b^{m \ldots k_r}_{i_1 \ldots i_p} - \ldots - \frac{\partial v^{k_r}}{\partial x^m} b^{k_1 \ldots m}_{i_1 \ldots i_p} \ . \tag{6}$$

The first line above contains terms one recognizes in the standard convective derivative. The terms in line (5) show the effect of covariant components of the tensor, while those in line (6) capture the effects of contravariant terms. As an example, apply the above procedure for the conservation of mass. The

density in the Eulerian frame $\rho(\vec{x}, t)$ is a scalar function, linked to the density $\bar{\rho}(\vec{\xi}, t)$ in the Lagrangian frame by $\bar{\rho} = J\rho$, hence density has a weight $W = 1$. In the Lagrangian frame conservation of mass states

$$\frac{D(\bar{\rho}/J)}{Dt} = 0. \tag{7}$$

By the Oldroyd theorem (4), the equivalent statement in the Eulerian frame

$$\frac{\delta\rho}{\delta t} = 0 \ . \tag{8}$$

The $\delta/\delta t$ derivative of a scalar field with weight $W = 1$ is

$$\frac{\delta\rho}{\delta t} = \frac{\partial\rho}{\partial t} + v^m \frac{\partial\rho}{\partial x^m} + \frac{\partial v^m}{\partial x^m}\rho \ , \tag{9}$$

and we obtain the familiar continuity equation in Eulerian coordinates, $\rho_t + \nabla \cdot (\rho\vec{v}) = 0$.

2.1.1 Oldroyd-B equations of motion

In his 1950 paper Oldroyd considers the Fröhlich and Sack [4] incompressible viscoelastic model which can be expressed in the co-deforming Lagrangian frame as

$$\left(1 + \lambda\frac{D}{Dt}\right)\boldsymbol{\pi}' = \eta\left(1 + \lambda'\frac{D}{Dt}\right)\boldsymbol{\varepsilon}^{(1)} \ , \tag{10}$$

where $\boldsymbol{\pi}'$ is the deviatoric part of the stress $\boldsymbol{\pi}$, with components $\pi'_{jk} = \pi_{jk} - \frac{1}{3}\pi^m_m \gamma_{jk}$ and $\boldsymbol{\varepsilon}^{(1)}$ is the rate of strain tensor with components $\varepsilon^{(1)}_{jk} = (v_{j,k} + v_{k,j})$ in the small deformation regime initially considered by Fröhlich and Sack. In the above, λ is the characteristic relaxation time and λ' is the characteristic retardation time. Transforming the above constitutive relation to a fixed Eulerian reference frame gives

$$\left(1 + \lambda \frac{\delta}{\delta t}\right) \boldsymbol{p}' = \eta \left(1 + \lambda' \frac{\delta}{\delta t}\right) \boldsymbol{e}^{(1)} \tag{11}$$

with $\boldsymbol{p}'$, $\boldsymbol{e}^{(1)}$ denoting the deviatoric stress and rate of strain tensor in the Eulerian frame. For polymeric solutions it is convenient to separate the total viscosity η into a polymeric and solvent part as in $\eta = \eta_s + \eta_p$. These are related to the characteristic times λ, λ' by $\lambda \eta_s = \lambda'(\eta_s + \eta_p)$ (see p. 37, [15]). The total deviatoric stress $\boldsymbol{p}'$ can be decomposed as

$$\boldsymbol{p}' = \eta_s \boldsymbol{e}^{(1)} + \boldsymbol{\tau} \ , \tag{12}$$

with the first part $\eta_s \boldsymbol{e}^{(1)}$ due to a Newtonian solvent, and the second part $\boldsymbol{\tau}$ due to the polymer. This leads to the relation

$$\left(1 + \lambda \frac{\delta}{\delta t}\right) \boldsymbol{\tau} = \eta_p \boldsymbol{e}^{(1)} \ . \tag{13}$$

The notation

$$\overset{\triangledown}{\boldsymbol{\tau}} = \frac{\delta \boldsymbol{\tau}}{\delta t} \tag{14}$$

is often used in the literature when $\boldsymbol{\tau}$ is a 2-contravariant tensor. Applying the Oldroyd theorem for this case leads to

$$\overset{\nabla}{\boldsymbol{\tau}} \;=\; \frac{\partial \boldsymbol{\tau}}{\partial t} + (\vec{v}\cdot\nabla)\,\boldsymbol{\tau} - (\nabla\vec{v})^T\;\boldsymbol{\tau} - \boldsymbol{\tau}\;(\nabla\vec{v})\;. \tag{15}$$

The additional stress exerted by the polymer is included as a force term on the solvent and we can write the following equations of motion

$$\nabla\cdot\vec{v}\;=0\;, \tag{16}$$

$$\frac{\partial\vec{v}}{\partial t} + (\vec{v}\cdot\nabla)\vec{v} = \frac{1}{\rho}\nabla\cdot(-p\mathbf{I}+\boldsymbol{\tau}) + \frac{\eta_s}{\rho}\nabla^2\vec{v}\;, \tag{17}$$

$$\overset{\nabla}{\boldsymbol{\tau}} \;= -\frac{1}{\lambda_1}\boldsymbol{\tau} + \frac{\eta_p}{\lambda_1}\boldsymbol{e}^{(1)}\;, \tag{18}$$

known as the Oldroyd-B system. If $\boldsymbol{\tau}=0$ at all times the above reduces to the Navier-Stokes equations for a Newtonian fluid. In component form the equations are

$$v_{k,k} = 0\;, \tag{19}$$

$$\partial_t v_i + v_j v_{i,j} = \frac{1}{\rho}\left(-p_{,i} + \tau_{ji,j}\right) + \frac{\eta_s}{\rho}v_{i,jj}\;, \tag{20}$$

$$\partial_t\tau_{ij} + v_k\tau_{ij,k} - v_{i,k}\tau_{kj} - \tau_{ik}v_{j,k} = \frac{\eta_p}{\lambda}\left(v_{j,i}+v_{i,j}\right) - \frac{1}{\lambda}\tau_{ij}\;. \tag{21}$$

The non-dimensional form of the momentum and stress evolution equations is

$$\frac{\partial\vec{v}}{\partial t} + (\vec{v}\cdot\nabla)\vec{v} = \nabla\cdot(-p\mathbf{I}+\boldsymbol{\tau}) + \frac{1}{Re}\nabla^2\vec{v}\;, \tag{22}$$

$$\overset{\nabla}{\boldsymbol{\tau}} = \frac{1}{We}\left(-\boldsymbol{\tau} + \frac{\eta_p}{\eta_s}\boldsymbol{e}^{(1)}\right), \tag{23}$$

with

$$Re = \frac{UL\rho}{\eta_s},\ We = \frac{\lambda U}{L}, \tag{24}$$

the Reynolds and Weissenberg numbers, respectively.

The rather complicated nature of the differentiation operation $\overset{\nabla}{\boldsymbol{\tau}}$ should not obscure the fact that the physical content of (18) is exactly the same as in the Fröhlich-Sack model (10). Of particular relevance to the main point of this paper is that the incompressibility condition constrains not only the evolution of the velocity field but also that of the additional stress due to viscoelastic effects. But rather than investigating the nature of such constraints in the Eulerian frame, it is simpler and more physically intuitive to do so in the Lagrangian frame using (10).

2.2 Elastic waves

A brief presentation of elastic waves in linear elastic solids is useful in analysis of wave modes for viscoelastic fluids. With $\vec{u}$ the elastic displacement vector and $\boldsymbol{e}^{(0)} = (\nabla\vec{u} + \nabla\vec{u}^T)$ the strain tensor, the stress in an elastic solid obeying Hooke's law is

$$s_{ik} = \frac{\nu E}{2(1+\nu)(1-2\nu)} e_{ll}\delta_{ik} + \frac{E}{2(1+\nu)} e_{ik}. \tag{25}$$

The equation of motion is

$$\ddot{u}_i = \frac{1}{\rho}\frac{\partial s_{ik}}{\partial x_k} = S^2\frac{\partial^2 u_i}{\partial x_k \partial x_k} + (P^2 - S^2)\frac{\partial^2 u_k}{\partial x_i \partial x_k} \ , \tag{26}$$

with the longitudinal and transverse wave speeds defined by

$$P^2 = \frac{E(1-\nu)}{\rho(1+\nu)(1-2\nu)} > S^2 = \frac{E}{2\rho(1+\nu)}. \tag{27}$$

Note that if the material is incompressible, the displacement field is constrained by the condition $\nabla \cdot \vec{u} = u_{k,k} = 0$ and the material can only support shear waves.

3 Numerical method

The Oldroyd-B system is a set of partial differential equations of mixed type (p. 54, [15]). A hyperbolic subsystem is associated with propagating shear waves and convective effects. The momentum diffusion is of parabolic character. The incompressibility condition imposes an overall elliptic constraint, such that a boundary value problem would have to be solved for all the flow variables at each time step. Such fully implicit discretizations have been carried out and have shown to be stable up to high Weissenberg or Deborah numbers (e.g. $De = 80$ in [14]). Solving the nonlinear system of equations arising from posing the boundary value problem is computationally expensive hence approaches which can reduce the amount of effort required are of

great interest. Several schemes have been proposed that combine a fractional in time or time-split method with a projection correction applied to the velocity field to enforce incompressibility ([12], [18]). The general approach to building a time-split scheme is presented by Owens & Phillips (p. 156-157, [15]) and consists of successively advancing in time the additional polymeric stress tensor $\boldsymbol{\tau}$, the velocity field $\vec{v}$ and finally correcting the velocity field.

3.1 Numerical splitting procedure

We now present an explicit time-split scheme. The distinguishing feature of the approach taken here is that the hyperbolic part is advanced forward in time taking into account the convective and shear wave mode eigenmodes naturally present in the system. A cell-centered finite-volume approach is adopted with $(\vec{v}^n, \boldsymbol{\tau}^n, p^n)$ the flow variable values at time t^n.

Stage 1: (From q^n to q^+). The following hyperbolic subsystem is used to obtain interim values $(\vec{v}^*, \boldsymbol{\tau}^*)$

$$\frac{\partial \vec{v}}{\partial t} + (\vec{v}\cdot\nabla)\vec{v} = \frac{1}{\rho}\nabla\cdot\boldsymbol{\tau} \ , \tag{28}$$

$$\overset{\nabla}{\boldsymbol{\tau}} = -\frac{1}{\lambda_1}\boldsymbol{\tau} + \frac{\eta_p}{\lambda_1}\boldsymbol{e}^{(1)} \ . \tag{29}$$

In component form for two dimensions the system can be written as

$$\frac{\partial q}{\partial t} + A\frac{\partial q}{\partial x} + B\frac{\partial q}{\partial y} = \psi(q) \tag{30}$$

with

$$q = \begin{bmatrix} v_x & v_y & \tau_{xx} & \tau_{xy} & \tau_{yy} \end{bmatrix}^T ,$$

$$A = \begin{bmatrix} v_x & 0 & -\frac{1}{\rho} & 0 & 0 \\ 0 & v_x & 0 & -\frac{1}{\rho} & 0 \\ -2\rho c_x^2 & 0 & v_x & 0 & 0 \\ -\tau_{xy} & -\rho c_x^2 & 0 & v_x & 0 \\ 0 & -2\tau_{xy} & 0 & 0 & v_x \end{bmatrix},$$

$$B = \begin{bmatrix} v_y & 0 & 0 & -\frac{1}{\rho} & 0 \\ 0 & v_y & 0 & 0 & -\frac{1}{\rho} \\ -2\tau_{xy} & 0 & v_y & 0 & 0 \\ -\rho c_y^2 & -\tau_{xy} & 0 & v_y & 0 \\ 0 & -2\rho c_y^2 & 0 & 0 & v_y \end{bmatrix},$$

$$\psi = \begin{bmatrix} 0 & 0 & -\tau_{xx}/\lambda & -\tau_{xy}/\lambda & -\tau_{yy}/\lambda \end{bmatrix}^T ,$$

$$\rho c_x^2 = \frac{\eta_p}{\lambda} + \tau_{xx},\ \rho c_y^2 = \frac{\eta_p}{\lambda} + \tau_{yy} \ .$$

The wave propagation approach of LeVeque [8] is used to advance system (30) forward in time. Briefly, in this approach the cell average values

$$\boldsymbol{Q}_{ij}^n = \frac{1}{h} \int_{x_{i-1/2}}^{x_{i+1/2}} \int_{y_{j-1/2}}^{y_{j+1/2}} \boldsymbol{q}(x, y, t^n)\ dx\ dy \ .$$

are used to define Riemann problems at each cell interface. To solve the Riemann problem, the jump at an interface is decomposed on the basis formed by eigenvectors of the A, B matrices. Consider the interface at $x_{i-1/2}$ and let $\bar{R}$ be the matrix of eigenvectors of A formed using the arithmetic average of cell center values to the left and right, $\bar{R} = R((Q^n_j + Q^n_{j-1})/2)$, $R = [r_1, r_2, r_3, r_4, r_5]$, $Ar_k = \lambda_k r_k$ for $k = 1, ..., 5$. The jump at the interface $\Delta Q^n_{i-1/2,j}$, is decomposed on the $\bar{R}$ eigenbasis

$$\Delta Q^n_{i-1/2,j} = Q^n_{i,j} - Q^n_{i,j-1} = \sum_{l=1}^{5} \alpha^l_{i-1/2,j} r^l_{i-1/2,j}.$$

The waves $\mathcal{W}^l_{i-1/2,j} = \alpha^l_{j-1/2} r^l_{j-1/2}$ propagate into cells to the left and right in accordance with the sign of the associated eigenvalue and modify the cell average values. For full details see [8]. The scheme is second order in time and space. The eigendecomposition of the A, B matrices is required to define the waves. For A the eigensystem is

$$\Lambda_A = diag(v_x - c_x\sqrt{2}, v_x - c_x, v_x, v_x + c_x, v_x + c_x\sqrt{2})$$

$$R_A = \begin{bmatrix} \rho c_x^3/\sqrt{2} & 0 & 0 & 0 & -\rho c_x^3/\sqrt{2} \\ c_x\tau_{xy}/\sqrt{2} & c_x & 0 & -c_x & -c_x\tau_{xy}/\sqrt{2} \\ \rho^2 c_x^4 & 0 & 0 & 0 & \rho^2 c_x^4 \\ \rho c_x^2\tau_{xy} & \rho c_x^2 & 0 & \rho c_x^2 & \rho c_x^2\tau_{xy} \\ \tau_{xy}^2 & 2\tau_{xy} & 1 & 2\tau_{xy} & \tau_{xy}^2 \end{bmatrix}$$

and the solution of the linear system $R_A\alpha = \Delta Q$ is given by

$$\begin{aligned} \alpha_1 &= \frac{1}{2c_x^4}\left(\Delta Q_3 + c_x\sqrt{2}\ \Delta Q_1\right),\ \alpha_5 = \frac{1}{2c_x^4}\left(\Delta Q_3 - c_x\sqrt{2}\ \Delta Q_1\right) \\ \alpha_2 &= \frac{1}{2c_x^4}\left[c_x^2\left(\Delta Q_4 + c_x\Delta Q_2\right) - \left(\Delta Q_3 + c_x\Delta Q_1\right)\tau_{xy}\right], \\ \alpha_4 &= \frac{1}{2c_x^4}\left[c_x^2(\Delta Q_4 - c_x\Delta Q_2) - (\Delta Q_3 - c_x\Delta Q_1)\tau_{xy}\right] \\ \alpha_3 &= \Delta Q_5 + \frac{\tau_{xy}}{c_x^4}\left(\tau_{xy}\Delta Q_3 - 2c_x^2\Delta Q_4\right), \end{aligned}$$

The eigensystem for B is

$$\Lambda = diag(v_y - c_y\sqrt{2}, v_y - c_y, v_y, v_y + c_y, v_y + c_y\sqrt{2})\ ,$$

$$R = \begin{bmatrix} c_y\tau_{xy}/\sqrt{2} & c_y & 0 & -c_y & -c_y\tau_{xy}/\sqrt{2} \\ \rho c_y^3/\sqrt{2} & 0 & 0 & 0 & -\rho c_y^3/\sqrt{2} \\ \tau_{xy}^2 & 2\tau_{xy} & 1 & 2\tau_{xy} & \tau_{xy}^2 \\ \rho c_y^2\tau_{xy} & \rho c_y^2 & 0 & \rho c_y^2 & \rho c_y^2\tau_{xy} \\ \rho^2 c_y^4 & 0 & 0 & 0 & \rho^2 c_y^4 \end{bmatrix}\ .$$

and the solution of $R_B\alpha = \Delta Q$ is

$$\alpha_1 = \frac{1}{2c_y^4}\left(\Delta Q_5 + c_y\sqrt{2}\Delta Q_2\right),\ \alpha_5 = \frac{1}{2c_y^4}\left(\Delta Q_5 - c_y\sqrt{2}\Delta Q_2\right), \tag{31}$$

$$\alpha_2 = \frac{1}{2c_y^4}\left[c_y^2\left(\Delta Q_4 + c_y\Delta Q_1\right) - \left(\Delta Q_5 + c_y\Delta Q_2\right)\tau_{xy}\right], \tag{32}$$

$$\alpha_4 = \frac{1}{2c_y^4}\left[c_y^2\left(\Delta Q_4 - c_y\Delta Q_1\right) - \left(\Delta Q_5 - c_y\Delta Q_2\right)\tau_{xy}\right], \tag{33}$$

$$\alpha_3 = \Delta Q_3 + \frac{\tau_{xy}}{c_y^4}(\tau_{xy}\Delta Q_5 - 2c_y^2\Delta Q_4)\ . \tag{34}$$

The source term $\psi(q)$ is included through Strang splitting.

Note that the eigensystem for each matrix contains three types of waves. For the A matrix we have: (1) longitudinal or P-waves of speed $v_x \pm \sqrt{2}c_x$, (2) shear or S-waves of speed $v_x \pm c_x$, and (3) a jump in the orthogonal normal stress τ_{yy} convected at the fluid velocity v_x. Though the full system of equations is incompressible and P-waves cannot appear, the reduced system (30) above exhibits P-waves since it does not contain the incompressibility condition. Indeed the hyperbolicity of (30) depends crucially on the presence of P-waves.

In the DPM to be presented below an additional stage will be introduced which will obtain field values q^+ from q^*. For now, we just set $(\vec{v}^+, \boldsymbol{\tau}^+) = (\vec{v}^*, \boldsymbol{\tau}^*)$. In this time-split method no further corrections of the stress are carried out, so we set $\boldsymbol{\tau}^{n+1} = \boldsymbol{\tau}^+$.

Stage 2: (From q^+ to q^{**}). A Crank-Nicolson procedure is employed to

compute viscous effects modeled by the subsystem

$$\frac{\partial \vec{v}}{\partial t} = \frac{\eta_s}{\rho} \nabla^2 \vec{v} \ , \tag{35}$$

thus obtaining a new velocity field $\vec{v}^{**}$ from the interim field $\vec{v}^{+}$. The numerical update is given by

$$\left(I - \frac{\Delta t \ \eta_s}{\rho} \nabla^2 \right) \vec{v}^{**} = \left(I + \frac{\Delta t \ \eta_s}{\rho} \nabla^2 \right) \vec{v}^{+}, \tag{36}$$

and the resulting system of linear equations is solved using a multigrid procedure.

Stage 3: (From q^{**} to q^{n+1}). A projection method is applied to correct the velocity field. In its simplest, first-order accurate in time form, the update is given by

$$\vec{v}^{n+1} = \vec{v}^{**} + \nabla p^{n+1} \ . \tag{37}$$

The correction potential is obtained by a multigrid solve of the Poisson equation

$$\nabla^2 p^{n+1} = -\frac{1}{\Delta t} \nabla \cdot \vec{v}^{**} \ . \tag{38}$$

The projection can be extended to second-order accuracy as shown by Van Kan [19] and Bell et al. [1], taking care to correctly apply time-split boundary conditions [2]. Before considering such extensions we turn to an investigation of the consequences of not enforcing the compressibility constraint in the evolution equation for $\boldsymbol{\tau}$.

3.2 Spurious modes

The above time-split approach is often encountered in numerical computations of Oldroyd-B. The specific details vary scheme to scheme. For example Trebotich et al. [18] and Webster et al. [20] use a Lax-Wendroff method to advance the viscoelastic stress. A fundamental distinction can be made between explicit methods that use an interim value of the viscoelastic stress in the momentum update enforcing incompressibility only on the velocity field and fully implicit schemes (e.g. [14]) that enforce the incompressibility constraint in the computation of $\boldsymbol{\tau}$ also.

It is perhaps useful to recall how the projection method functions for the Navier-Stokes equations. To restrict the presentation to the essential idea, a first order scheme is discussed. Starting from the velocity and pressure fields $(\vec{v}^n, p^n)$ at time t^n the momentum equation is used to construct an interim velocity field $\vec{v}^*$. In component form

$$v_i^* = v_i^n + \Delta t \left[-v_j^n v_{i,j}^n + \eta_s v_{i,jj} \right] \ . \tag{39}$$

Taking the divergence gives

$$v_{i,i}^* = -\Delta t \ v_{j,i}^n v_{i,j}^n \ , \tag{40}$$

which we can interpret as stating that the nonlinear terms arising from the convective derivative do not preserve divergence-free velocity fields. Nu-

merical approximations of the differential operations in (39) can lead to further divergence errors. The projection correction for Navier-Stokes computes $v_i^{n+1} = v_i^* + \phi_{,i}$, with ϕ the solution of $\phi_{,jj} = -v_{k,k}/\Delta t$.

Schemes for the Oldroyd-B model that advance the viscoelastic stress independently of the incompressibility constraint lead to the same type of error. The nonlinear convective terms present in the $\overset{\nabla}{\boldsymbol{\tau}}$ derivative can lead to stresses associated with P-waves (longitudinal modes) that are prohibited by the incompressibility constraint. If the interim stress value $\boldsymbol{\tau}^*$ is subsequently used in the momentum update a spurious force acts upon the fluid. Subsequent correction of the velocity field by a projection method will enforce compressibility *after* the action of this spurious force field and, in general, will not remove the effects of the spurious forces.

We present now a diagnosis of the appearance of longitudinal modes in the viscoelastic stress. A symmetric tensor stress $\boldsymbol{\tau}^*$ function defined on some domain Ω can always be decomposed into a divergence-free part $\boldsymbol{\beta}$, which does not carry any forces, and a force-carrying part $\boldsymbol{\alpha}$

$$\boldsymbol{\tau}^* = \boldsymbol{\alpha}^* + \boldsymbol{\beta}^* \ . \tag{41}$$

The divergence-free part satisfies the equations

$$\nabla \cdot \boldsymbol{\beta}^* = 0 \text{ in } \Omega \tag{42}$$

$$\boldsymbol{\beta}^* \cdot \vec{n} = 0 \text{ on } \partial\Omega. \tag{43}$$

The force-carrying part can be represented as

$$\boldsymbol{\alpha}^* = \nabla\vec{u} + (\nabla\vec{u}^*)^T \ , \tag{44}$$

with the vector field $\vec{u}$ computed by solving the elliptic system

$$\begin{aligned} \nabla^2\vec{u}^* + \nabla(\nabla\cdot\vec{u}^*) &= \nabla\cdot\boldsymbol{\tau}^* \ \text{ in } \Omega \ , \\ \left[\nabla\vec{u}^* + (\nabla\vec{u}^*)^T\right]\cdot\vec{n} &= -\boldsymbol{\tau}^*\cdot\vec{n} \text{ on } \partial\Omega. \end{aligned} \tag{45}$$

Note that the link between $\boldsymbol{\alpha}^*$ and $\vec{u}^*$ is of the same form as that given by the Fröhlich-Sack model (10). The time dependence in (10) implies a link between the stress and the entire time-deformation history so $\vec{u}^*$ which is determined here for $\boldsymbol{\tau}^*$ at just one instant in time cannot be identified as the actual deformation field of the viscoelastic material. However, since the viscoelastic deformation field was subject to the incompressibility constraint at all times, the field $\vec{u}^*$ must reflect this constraint and the solution of (45) should satisfy

$$\nabla\cdot\vec{u}^* = 0 \ , \tag{46}$$

if the stress field $\boldsymbol{\tau}^*$ has been evolved correctly by a numerical scheme. We proceed to verify whether the condition (46) is met by the time-split scheme.

A computation of the flow inside a square cavity of unit side length is presented in Fig. 1. The top lid moves at velocity $U = 1$, the Weissenberg number is $We = 0.1$ and the Reynolds number is $Re = 1$. The time-split

method presented above was used on a 100x100 grid. The flow is shown at $t = 4$ and is steady state. The viscoelastic stress field was decomposed into divergence-free and force-carrying parts and the divergence of $\vec{u}$ from (44) is shown as contour lines using a logarithmic scale. Clearly $\vec{u}^*$ is not divergence-free.

The pseudo-deformation field $\vec{u}^*$ can be separated into a divergence-free part ($\vec{w}^*$) and the gradient of a scalar potential using a Helmholtz decomposition

$$\vec{u}^* = \nabla\varphi^* + \vec{w}^* \ , \tag{47}$$

with φ^* computed by solving the Poisson equation $\nabla^2\varphi^* = \nabla\cdot\ \vec{u}^*$. The $\nabla\cdot\boldsymbol{\tau}^*$ term is the viscoelastic force used in the momentum equation. The forces induced by the divergence carrying part of $\vec{u}$ are spurious and given by

$$\vec{f'} = \nabla\cdot\boldsymbol{\tau'} = \nabla(\vec{u}^* - \vec{w}^*) + \nabla(\vec{u}^* - \vec{w}^*)^T \ . \tag{48}$$

The $\boldsymbol{\tau}'$ field is presented in Fig. 2 along with the velocity field obtained for a computation at higher Weissenberg number $We = 0.30$ and Reynolds number of $Re = 1$ at $t = 0.4$. A steady flow regime is expected for these parameter values from experimental results [16]. We surmise that the spurious forces are leading to a non-physical loss of flow stability. The numerical computations for this case did not diverge and the computation could be advanced to later times (the computation up to $t = 10$ was carried out).

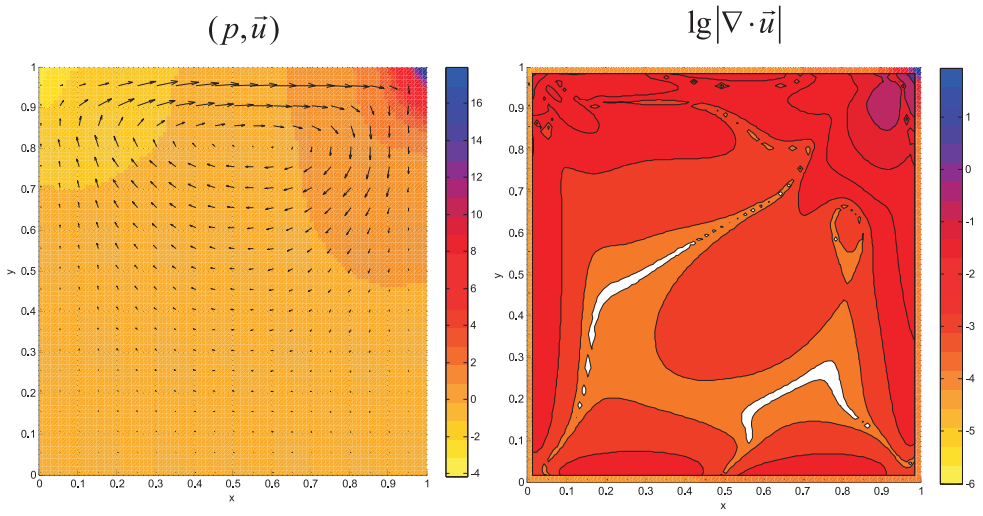

Figure 1: Cavity flow at $Re = 1$, $We = 0.1$ and contour lines of the divergence of the pseudo-deformation field u

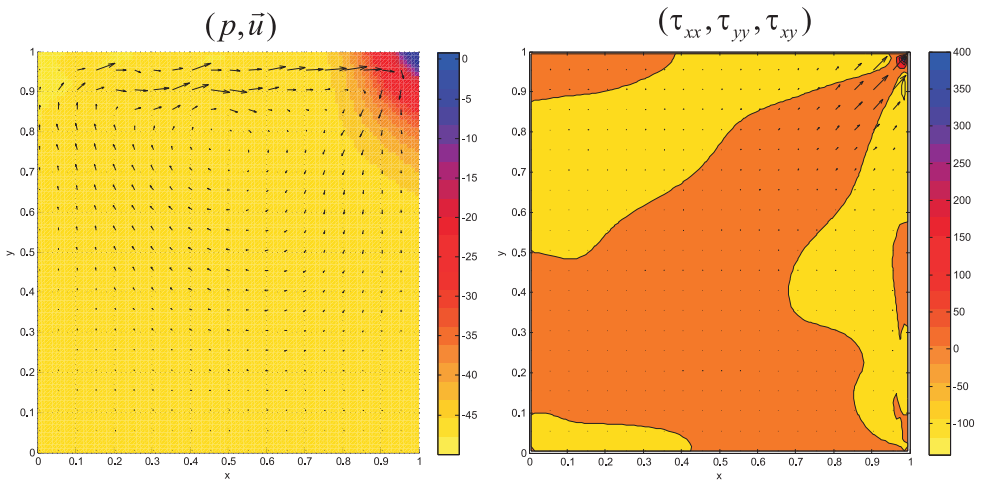

Figure 2: Non-physical oscillations in cavity flow at $Re = 1$, $We = 0.3$ and a representation of the spurious longitudinal stress field $\boldsymbol{\tau}'$

3.3 Relevance to the high Weissenberg number problem

The loss of numerical or physical stability at high Weissenberg numbers has been observed in numerical simulations of viscoelastic flows for some time. A good overview of the history of the problem is presented by Owens and Phillips (p. 173, [15]). The improper treatment of hyperbolic terms in steady-state computations has been identified as a major source of error and proper upwinding has led to stable computations for both unsteady and steady flows at relatively high Weissenberg numbers [18]. Implicit algorithms have been shown to behave more stably than explicit schemes [14]. The main contribution of this paper is that part of the observed difficulties in explicit time-split schemes can be traced to a numerical approximation of the viscoelastic stress that does not conform to the constraints imposed by the incompressibility condition, in particular that longitudinal modes and associated forces should not arise in the fluid.

4 Double projection method

Based on the above observations we now introduce a correction of the interim stress field $\boldsymbol{\tau}^*$ obtained at the end of Stage 1 of the time-split method presented in Sect 3.

Stage 1a: (From q^* to q^+). One of the attractive properties of the wave propagation approach used above is the close connection between numerical

model and physical behavior. We wish to maintain this approach and continue updating the velocity and stress fields simultaneously. The spurious forces have furnished an erroneous prediction of the velocity field. Hence we introduce one more stage and correct the viscoelastic stress by subtracting the part associated with longitudinal modes

$$\boldsymbol{\tau}^{+} = \nabla(\vec{w}^{*}) + \nabla(\vec{w}^{*})^{T} \tag{49}$$

with $\vec{w}^{*}$ determined from

$$\vec{w}^{*} = \vec{u}^{*} - \nabla\varphi^{*} \tag{50}$$

In order to compute the corrected stress field the elliptic problems

$$\nabla^{2}\vec{u}^{*} + \nabla(\nabla\cdot\vec{u}^{*}) = \nabla\cdot\boldsymbol{\tau}^{*} \ \text{ in } \Omega \tag{51}$$
$$\left[\nabla\vec{u}^{*} + (\nabla\vec{u}^{*})^{T}\right]\cdot\vec{n} = -\boldsymbol{\tau}^{*}\cdot\vec{n} \text{ on } \partial\Omega,$$

and

$$\nabla^{2}\varphi^{*} = \nabla\cdot\ \vec{u}^{*} \ \text{ in } \Omega \tag{52}$$
$$\varphi^{*} = 0 \text{ on } \partial\Omega, \tag{53}$$

are solved. This is the first projection of the Double Projection Method proposed here. Note that we are correcting a two-component tensor. Hence it is to be expected that at least a vector potential (in this case $\vec{w}^{*}$) is required

to remove the longitudinal modes.

The velocity field has already been updated using the $\boldsymbol{\tau}^*$ viscoelastic stress in Stage 1. We correct the velocity field using the equation

$$\vec{v}_t = \nabla \cdot (\boldsymbol{\tau}^+ - \boldsymbol{\tau}^*) \ . \tag{54}$$

Using a second-order midpoint rule and taking into account that at the beginning of the time step the stress is assumed to contain no longitudinal modes the discrete update is

$$\vec{v}^+ = \vec{v}^* + \frac{\Delta t}{2} \nabla \cdot (\boldsymbol{\tau}^+ - \boldsymbol{\tau}^*) \ . \tag{55}$$

Algorithm complexity. Stages 1, 2 and 3 of the Double Projection Method are the same as the time split method from Sect. 3. Overall for a 2D computation we shall solve 4 scalar elliptic equations. This should be compared to a fully implicit method in which 6 equations are simultaneously solved. In 3D the DPM requires solving 5 scalar as opposed to 10 equations required for a fully implicit procedure. In practice the corrections have been found to within relative error of 10^{-6} in only 1 multigrid V-cycle since a very good initial approximation is available from the previous time step.

4.1 Comparison to standard projection algorithm

A natural question to ask is whether there is any difference in the velocity field predicted by the double projection method by comparison to that obtained by applying a single projection step. To answer this question we carry out a computation in Fourier space. Let

$$\vec{V}(\vec{k},t) = \int_{-\infty}^{+\infty} \vec{v}(x,t) e^{-i\vec{k}\cdot\vec{x}}\, d\vec{x} \tag{56}$$

In a single projection method the interim velocity field $\vec{v}^*$ is modified by the gradient of a scalar potential ϕ_1 to obtained a corrected field $\vec{v}_1$

$$\vec{v}_1 = \vec{v}^* + \nabla\phi_1,\ \nabla^2\phi_1 = -\nabla\cdot\vec{v}^*\ . \tag{57}$$

Let Φ be the Fourier transform of ϕ. Solving the above Poisson equation leads to $\Phi = i(\vec{k}\cdot\vec{V}^*)/k^2$. In Fourier space the correction to the velocity field is given by

$$\vec{V}_1 = \vec{V}^* - \frac{(\vec{k}\cdot\vec{V}^*)}{k^2}\vec{k}\ . \tag{58}$$

Incidentally, the above form clearly shows that the correction is indeed a projection along the $\vec{k}$ direction. In the double projection method we would start from the same interim velocity field $\vec{v}^*$. Consider the case of explicit Euler time stepping for simplicity. Removing the effect of longitudinal modes

leads to the correction

$$\vec{v}^{+} = \vec{v}^{*} + \frac{\Delta t}{2}\left[\nabla^2 \vec{u}^{n+1} - \nabla^2 \vec{u}^{*} - \nabla(\nabla \cdot \vec{u}^{*})\right] \ , \tag{59}$$

which in Fourier space becomes

$$\vec{V}^{+} = \vec{V}^{*} + \frac{\Delta t}{2}\left[-k^2\left(\vec{U}^{n+1} - \vec{U}^{*}\right) + (\vec{k}\cdot\vec{U}^{*})\vec{k}\right] \ . \tag{60}$$

The final velocity field is obtained by the second projection step

$$\vec{V}_2 = \vec{V}^{+} - \frac{(\vec{k}\cdot\vec{V}^{+})}{k^2}\vec{k} \ . \tag{61}$$

Computing the difference between the velocity fields predicted by the two methods gives

$$\Delta\vec{V} = \vec{V}_2 - \vec{V}_1 = -\frac{\Delta t}{2}\left[k^2\left(\vec{U}^{n+1} - \vec{U}^{*}\right) + (\vec{k}\cdot\vec{U}^{*})\vec{k}\right] \ . \tag{62}$$

If the interim deformation field would have been divergence-free, then $\vec{k}\cdot\vec{U}^{*} = 0$ and $\vec{U}^{n+1} = \vec{U}^{*}$, and there would be no difference between the double projection method and standard projection. If the interim deformation field is not divergence-free, we see that the predictions given by the standard projection method differ from those of the double projection method. As expected, the difference $\Delta\vec{V}$ is a divergence free-field, $\Delta\vec{V}\cdot\vec{k} = 0$.

5 Numerical results

5.1 Cavity problem

We conclude by comparing numerical computations to experimental results. The numerical computations were carried in the first author's well tested BEARCLAW package. The wave propagation algorithm and linear solvers used in the DPM algorithm have shown robust second-order convergence for a number of problems.

In all cases computed here the Reynolds number is $Re = 1$. Fig. 3-5 present stable steady solutions obtained by the DPM for $We = 0.075, 0.15, 0.075$ in comparison with experimental visualizations from [16]. Good qualitative agreement with the experimental results is observed.

6 Conclusions

Numerical methods benefit from incorporating physical knowledge about the system being modeled. In this paper the utility of gaining insight by considering the physical evolution of a viscoelastic model in the co-moving, co-deforming Lagrangian frame of reference has been highlighted. The observation that the viscoelastic field should exhibit no longitudinal modes led to an investigation of whether standard time-split approaches maintain this restriction. A prototypical method has been found to violate this constraint and a correction has been proposed in the form of an additional projection

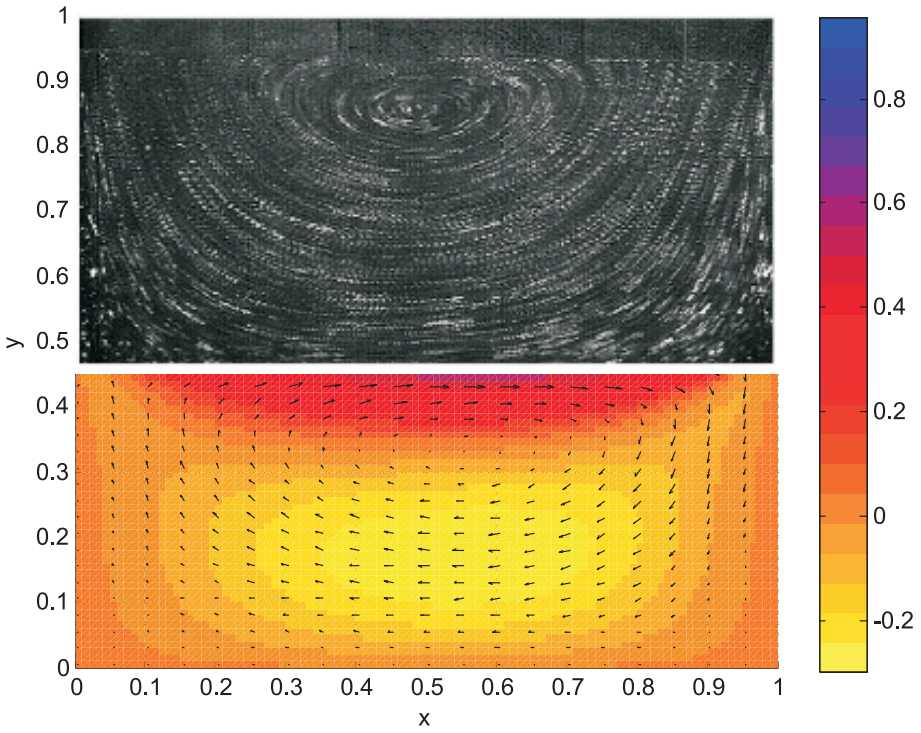

Figure 3: Comparison of computed viscoelastic cavity flow for an Oldroyd-B fluid at $We = 0.3$ using the double projection method with the experimental results of Pakdel et al. [16]

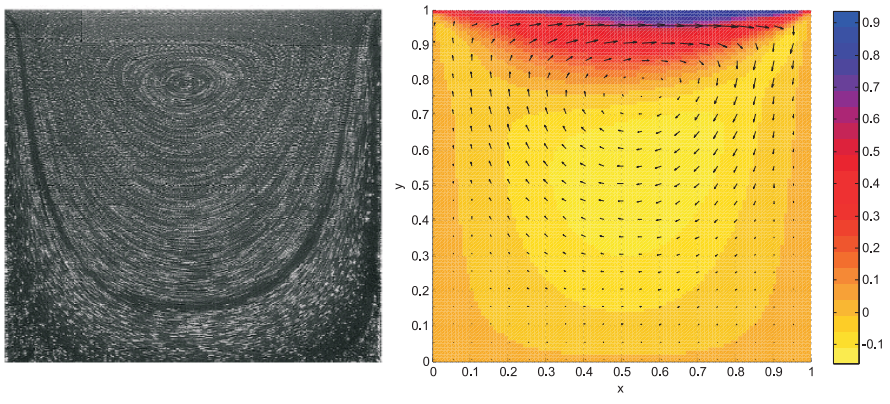

Figure 4: As before, but for $We = 0.15$

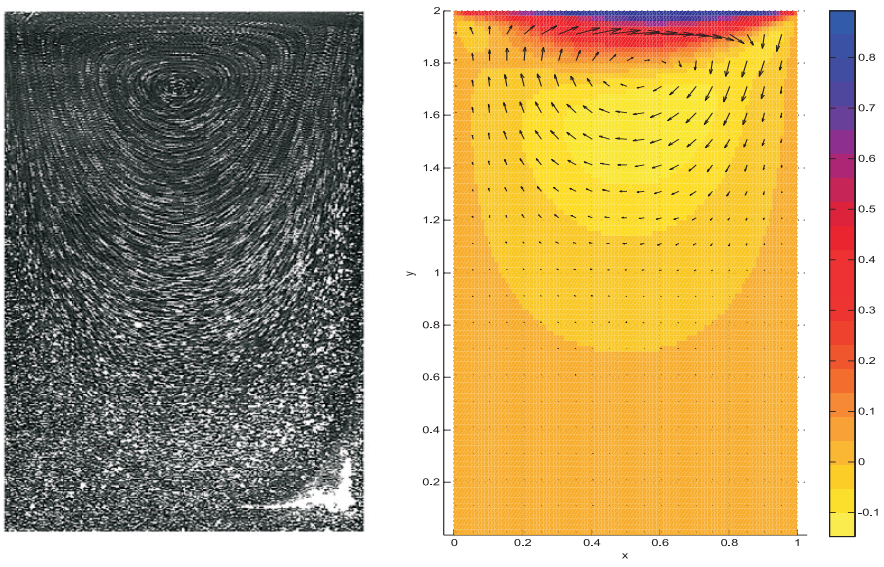

Figure 5: As before, but for $We = 0.075$

step that eliminates spurious longitudinal forces from the viscoelastic stress field.

Computations on the cavity problem have shown that the Double Projection Method (DPM) introduced here stabilizes computations that exhibit non-physical oscillations in the time-split method which uses a projection only to correct the velocity field. Furthermore, the additional correction furnished by the DPM has been shown to be essentially different from that given by the velocity projection step as detailed in equation (62). The fully explicit first stage of the algorithm used here perhaps introduces larger longitudinal force errors than predictor-corrector algorithms used in other schemes [18], and the effects pointed out here might be less acute for other algorithms. Nonetheless, all explicit methods would in general introduce spurious longi-

tudinal modes in the viscoelastic stress tensor and can be corrected using the additional projection step proposed here. In this sense, the correction is general and can be integrated into different algorithms for the computation of unsteady viscoelastic flows.

Further research directions are immediately suggested by this work and are being pursued. Similar to the divergence-cleaning procedures in magnetohydrodynamic computations, different approaches can be attempted here. In particular, numerical schemes that are guaranteed not to introduce longitudinal modes are being investigated in order to obtain a constrained-transport type scheme. Though the DPM method has been introduced and exemplified for an Oldroyd-B fluid, the procedure should be relevant for any incompressible viscoelastic fluid and extensions of the procedure to FENE-P type fluids are underway.

Acknowledgements. This work was motivated by viscoelastic biological flows suggested from the University of North Carolina *Virtual Lung Project* and partially supported by NIH grant R01-HL077546-01A2.

References

[1] J.B. Bell, P. Colella, H.M. Glaz, A 2nd-order accurate projection method for the incompressible Navier-Stokes equations, J. Comp. Phys. 85(1989) 257-283.

[2] D. Brown, R. Cortez, M. Minion, Accurate projection methods for the

incompressible Navier-Stokes equations, J. Comp. Phys. 168 (2001) 464–499.

[3] A. J. Chorin, Numerical solutions of the Navier-Stokes equations, Math. Comp. 22(1968) 745-762.

[4] H. Fröhlich, R.A. Sack, Theory of the rheological properties of dispersions, Proc. Roy. Soc. London A185 (1946) 415-430.

[5] M. Gerritsma, Time dependent numerical simulations of a viscoelastic fluid on a staggered grid, PhD thesis, 1996.

[6] H. Hencky, Die Bewegungsgleichungen beim nichtstationären Fliessen plastischer Massen, ZaMM (1925) 144-146.

[7] R. Kupferman, Simulation of viscoelastic fluids: Couette-Taylor flow, J. Comp. Phys., 147(1998) 22-59.

[8] R. J. LeVeque, Wave propagation algorithms for multi-dimensional hyperbolic systems, J. Comp. Phys., 131(1997) 327-353.

[9] A.S. Lodge, Elastic Liquids, Academic Press (New York, 1964).

[10] A.S. Lodge, Body tensors in continuum mechanics, Academic Press (New York, 1974)

[11] C. Macosko, Rheology: Principles, Measurements and Applications, Wiley Publishers, 1994.

[12] H. Matallah, P. Townsend, M.F. Webster, Recovery and stress-splitting schemes for viscoelastic flows, J. Non-Newtonian Fl. Mech. 75 (1998) 139-166.

[13] J.G. Oldroyd, On the formulation of rheological equations of state, Proc. Roy. Soc. London A200(1950) 523-541.

[14] P.J. Oliveira, Method for time-dependent simulations of viscoelastic flows: vortex shedding behind cylinder, J. Non-Newtonian Fl. Mech. 101(2001) 113-137.

[15] R. G. Owens, T. N. Phillips, Computational Rheology, Imperial College Press, 2002.

[16] P. Pakdel, S.H. Spiegelberg, G.H. McKinley, Cavity flows of elastic liquids: two-dimensional flows, Phys. Fl. 9(1997) 3123-3140.

[17] R. Temam, Sur l'approximation de la solution des équations de Navier-Stokes par la méthode de pas fractionnaires, Arch. Rat. Mech. Anal. 33(1969) 377-385.

[18] D. Trebotich, P. Collela, G.H. Miller, A stable and convergent scheme for viscoelastic flow in contraction channels, J. Comp. Phys., 205(2005) 315-342.

[19] J. Van Kan, A second-order accurate presure-correction scheme for viscous incompressible flow, SIAM J. Sci. Comput. 3(1986) 870-891.

[20] M.F. Webster, H.R. Tamaddon-Jahromi, M. Aboubacar, Transient viscoelastic flows in planar contractions, J. Non-Newtonian Fluid Mech. 118(2004) 83-101.